

Supersonic Transitional Airfoil Shapes of Minimum Drag

A. V. Fedorov*

Moscow Institute of Physics and Technology, Zhukovski 140160, Russia
and

N. D. Malmuth†

Rockwell International Science Center, Thousand Oaks, California 91358

Feasibility of a procedure incorporating transition considerations in optimizing total drag has been demonstrated. The Schittkowski algorithm was modified to demonstrate the approach on two-dimensional airfoils. Cubic spline basis functions were used to describe the airfoils, and total drag (wave + friction) was minimized under the constraint of a fixed airfoil area. Reynolds numbers were assumed such that the airfoil was transitional, generally with the forward portion laminar and the aft turbulent. The transition locus was calculated using the fast transition prediction module, which provides rapid computation of the Tollmien–Schlichting wave amplification factor N and estimates transition point by the e^N method. The laminar friction drag was evaluated using self-similar solutions of the boundary-layer equations. The friction drag for the turbulent portion was computed assuming a one-seventh velocity profile. With this framework, the total drag was a function of the functional x_{tr} , the streamwise location of transition. As a validation of the method, the algorithm gave the correct global optimum for the inviscid case, which is the parabolic arc profile. For the viscous case, significantly different locations of the maximum thickness led to only small differences in the minimum total drag. In addition, the drag reductions from the optimal inviscid parabolic profile were about 10%. Convergence with respect to the number of spline knots was achieved. Important challenges were met to reduce the effect of truncation errors in the numerical approximation of differentiations such as those used in the evaluation of the Hessian matrix. Despite these difficulties, generalization of the approach to treat infinite yawed and swept wings accounting for suction, crossflow instabilities, and vortex drag appears feasible.

Nomenclature

C_f	= friction coefficient
C_p	= pressure coefficient
c	= airfoil chord
D	= drag
F	= airfoil shape function
h	= interval between knots
K	= number of knots
M	= freestream Mach number
N	= amplification ratio
p	= pressure
R_c	= chord Reynolds number, $c\rho_\infty u_\infty/\mu_\infty$
S	= airfoil area
T	= temperature
U	= freestream speed
u	= velocity in x direction
x, y, z	= Cartesian coordinates
γ	= specific heat ratio
δ_2	= momentum thickness
ε	= airfoil thickness ratio
ε_c	= curvature constraint parameter
Λ	= pressure gradient parameter
μ	= viscosity
ξ	= effective length
ρ	= density

Subscripts

e	= upper boundary-layer edge
f	= friction
lam	= laminar
t	= total
tr	= transition
turb	= turbulent
w	= wave
∞	= freestream quantity

I. Introduction

LOW drag is critical to the success of all types of aircraft, such as supersonic transports and fighters. For supersonic cruise vehicles, wave-induced and friction drag must be reduced. Wave drag is associated with the entropy gain through shock waves. Induced drag is related to the kinetic energy associated with the wake vortex system, and friction drag is related to dissipation in the boundary layer. Beneficial interference (Busemann biplane), variable sweep, and area ruling exemplify wave drag reduction approaches. For low vortex drag, favorable span loading is desired. For planar configurations such as thin wings, this is achieved by an elliptic span loading. Optimization twist, camber, and thickness are classical approaches used with linear procedures such as panel methods to design wings for minimum vortex and trim drag as well as good landing characteristics. Nonplanar arrangements such as biplanes lead to other solutions. Jones¹ has shown that an oblique wing can be beneficial. Friction drag can be reduced by replacing the turbulent portion of the boundary layer with laminar flow.

Inverse methods seeking a pressure distribution that will minimize wave drag, separation, and transition have received attention. In the inverse problem, the unknown is the body shape that supports a given pressure distribution, as contrasted to the direct problem in which the body shape is specified and the unknown is the pressure distribution. Mixed

Received Oct. 5, 1996; revision received June 9, 1997; accepted for publication June 9, 1997. Copyright © 1997 by A. V. Fedorov and N. D. Malmuth. Published by the American Institute of Aeronautics and Astronautics, Inc., with permission.

*Principal Researcher, Department of Aeromechanics and Flight Engineering, 16 Gagarin Street.

†Senior Scientist, Computational Fluid Dynamics Department, 1049 Camino Dos Rios. Fellow AIAA.

problems involving inverse and direct approaches can also be formulated. Recent examples of inverse approaches are in the transonic range.² Although these procedures have been used on airplanes such as subsonic transports, the solution may be suboptimal because the fairing that smooths the shock-induced pressure discontinuity may not eliminate shocks off the body or wave drag. Other issues that have not been resolved completely for nonlinear flows are the proper formulation of pressures that avoid trailing-edge openness or fishtailed sections.

These examples represent a reduction of the separate components of friction and pressure drag. The field of reduction of total drag involving the nonlinear interaction between friction and pressure drag is in its infancy. Current computational fluid dynamics (CFD) methods employing Reynolds-averaged Navier–Stokes (RANS) solvers are receiving attention in this connection. Computational intensity and the lack of adequate transition modeling, as well as noise in the optimization method, are major issues even for new procedures such as adjoint, stimulated annealing, and genetic algorithms.^{3,4}

Another class of examples, supersonic laminar flow control (SLFC), has been proposed to augment aerodynamic efficiency of supersonic transports such as the High Speed Civil Transport (HSCT). Rapid techniques are needed to solve the special optimization problems associated with SLFC. For active laminar flow control involving a suction glove over a wing, it is necessary to determine the suction distribution that will prolong the laminar boundary-layer run while keeping wave and vortex drag under control. This amounts to minimizing the total drag as well as the pumping requirements and structural weight. Previous attempts at solving this problem used an inverse method for the design of the suction system, considering the impact on wave drag afterward. A less ambitious optimization problem that is a challenge to optimizers with RANS constraints is to consider the role of laminar–turbulent transition in the reduction of total drag.

This paper introduces a methodology that will be used to solve such problems. It contains an optimization approach whose feasibility is demonstrated on two-dimensional supersonic airfoils. This is the forerunner of generalizations to swept wings including suction. A major feature is the use of a fast transition prediction module (TPM) (Ref. 5) that accelerates the optimization process for use in a desktop computing environment. Preliminary results from the method are discussed as is a plan for generalizing its applicability. Reference 6 determines optimum suction that maximizes laminar run without consideration of drag. The approach that is applied herein is the first to address the minimization of total drag accounting for transition.

II. Analysis

A. Inviscid Flow

Inviscid flow over a thin airfoil with sharp leading edges is considered at zero angle of attack. Flow parameters are non-dimensionalized using their freestream values. The airfoil shape is specified as

$$\bar{y}(\bar{x}) = \varepsilon \bar{F}(\bar{x}) \quad (1)$$

where the coordinates \bar{x} and \bar{y} are nondimensionalized using airfoil chord c , ε is a small parameter characterizing the airfoil thickness ratio, and $\bar{F}(\bar{x}) = \mathcal{O}(1)$.

According to Ackeret's linearized theory, the pressure coefficient at a point \bar{x} of the upper surface is given by⁷

$$C_p \equiv \frac{2(p - p_\infty)}{\rho_\infty U_\infty^2} = 2\varepsilon \frac{\bar{F}'(\bar{x})}{\sqrt{M^2 - 1}} \quad (2)$$

where $\bar{F}' = d\bar{F}/d\bar{x}$. The streamwise velocity \bar{u} , temperature \bar{T} ,

and pressure \bar{p} at the upper boundary-layer edge are, respectively,

$$\bar{u} \equiv \frac{u_e}{U_\infty} = 1 - \varepsilon \frac{\bar{F}'(\bar{x})}{\sqrt{M^2 - 1}} + \mathcal{O}(\varepsilon^2) \quad (3)$$

$$\bar{T} \equiv \frac{T_e}{T_\infty} = 1 + \varepsilon \frac{(\gamma - 1)M^2 \bar{F}'(\bar{x})}{\sqrt{M^2 - 1}} + \mathcal{O}(\varepsilon^2) \quad (4)$$

$$\bar{p} \equiv \frac{p_e}{p_\infty} = 1 + \varepsilon \frac{\gamma M^2 \bar{F}'(\bar{x})}{\sqrt{M^2 - 1}} + \mathcal{O}(\varepsilon^2) \quad (5)$$

The pressure gradient, which is to be involved in computation of the transition point and friction drag, is characterized by the following parameter^{8,9}:

$$\Lambda \equiv \frac{2\xi}{u_e} \frac{du_e}{d\xi}, \quad \xi = \int_0^x \rho_e u_e \mu_e dx \quad (6)$$

where ξ is an effective length, and μ is calculated using the power law $\mu = T^m$, $m = 0.75$. From Eqs. (3–5), the parameter Λ is approximated as

$$\Lambda = -2\varepsilon \bar{x} \frac{\bar{F}''(\bar{x})}{\sqrt{M^2 - 1}} + \mathcal{O}(\varepsilon^2) \quad (7)$$

The wave drag \bar{D}_w is calculated using the following formula:

$$\bar{D}_w = \int_0^1 C_p \bar{y}'(\bar{x}) d\bar{x} = \frac{2\varepsilon^2}{\sqrt{M^2 - 1}} \int_0^1 [\bar{F}'(\bar{x})]^2 d\bar{x} + \mathcal{O}(\varepsilon^3) \quad (8)$$

B. Viscous Flow

The airfoil friction drag is defined as

$$\bar{D}_f(\bar{x}) = \int_0^{\bar{x}} C_f d\bar{x} \quad (9)$$

where C_f is friction coefficient of laminar or turbulent flow.

The laminar boundary-layer characteristics are calculated using the Lees–Dorodnitsyn transformation and the local similarity approximation of the boundary-layer equations.⁹ The laminar friction coefficient $C_{f,\text{lamin}}$ is calculated for the adiabatic wall condition at Prandtl number $Pr = 0.72$ and the specific heat ratio $\gamma = 1.4$.

The transition point x_{tr} is determined using the transition prediction module.⁵ This module provides fast calculations of the Tollmien–Schlichting wave growth rates and the amplification factor N . The transition point is predicted using the e^N method.^{10–15} In contrast to the local empirical correlation methods, the e^N method accounts for the history of the boundary-layer disturbance growth, which is important for airfoil shaping.

To estimate turbulent friction drag, we assume that turbulent flow occurs instantaneously at the transition onset point x_{tr} . Because the transitional region is neglected, the local friction coefficient jumps from laminar to fully turbulent value at x_{tr} . Since the turbulent boundary layer is less sensitive to pressure gradient than the laminar boundary layer, the turbulent friction coefficient of a thin airfoil can be estimated using a flat-plate approximation, given by Ref. 9 as

$$C_{f,\text{turb}}(x) = 0.058 R_l^{-1/5} (1 + 0.144 M_e^2)^{-0.65} \quad (10)$$

where $R_l = \rho_e u_e l / \mu_e$ is the local Reynolds number based on the length $l = x - x_{tr}$. Because the turbulent boundary layer does not begin at the leading edge, but appears at x_{tr} , the initial point x_i should be determined from the condition that the lam-

inar and turbulent momentum thicknesses are equal at x_{tr} .⁸ That leads to the following expression:

$$\bar{x}_i = \bar{x}_{tr} - \left[\frac{4}{5B} \delta_{2, \text{lam}}(\bar{x}_{tr}) \right]^{5/4} \quad (11)$$

$$B = 0.029 R_c^{-1/5} (1 + 0.144 M_c^2)^{-0.65}$$

Detailed derivation of this relation is given in Refs. 5 and 16. Summarizing, we obtain the following formula for the total drag \bar{D} :

$$\bar{D}_t = \frac{2\varepsilon^2}{\sqrt{M^2 - 1}} \int_0^1 [F'(\bar{x})]^2 d\bar{x} + \int_0^{\bar{x}_{tr}} C_{f, \text{lam}} d\bar{x} + \int_{\bar{x}_{tr}}^1 C_{f, \text{turb}}(\bar{x}) d\bar{x} \quad (12)$$

III. Minimum Drag Problem

Minimization of the airfoil drag can be considered for the isoperimetric constraint

$$\int_0^1 \bar{F}''(\bar{x}) d\bar{x} = \text{const} \quad (13)$$

If the profile area is prescribed ($n = 1$), the wing volume and the torsional stiffness of a thin-skin structure are given. If the moment of inertia of the airfoil contour with respect to the x axis is prescribed ($n = 2$), this is equivalent to prescribing the bending stiffness or the torsional stiffness of a thin-skin structure. If the moment of inertia of the profile area with respect to the x axis is prescribed ($n = 3$), this is equivalent to specifying the bending stiffness or the torsional stiffness of a solid section wing.

The minimum drag problem can be stated as follows. Problem A: in the $\bar{F}(\bar{x})$ class of functions, which are consistent with the sharp leading-edge conditions $\bar{F}(0) = \bar{F}(1) = 0$ and the isoperimetric constraint [Eq. (13)], find the particular function that minimizes \bar{D}_n given by Eq. (12).

If the friction drag is neglected, problem A has analytical solutions given in Ref. 17. For example, the optimum shape for a given profile area ($n = 1$) is the parabolic arc

$$\bar{y}(\bar{x}) = \varepsilon \bar{F}(\bar{x}), \quad \bar{F}(\bar{x}) = 2\bar{x}(1 - \bar{x}) \quad (14)$$

If the friction drag is involved in the analysis, an optimum shape cannot be found analytically because of the complex dependence of the friction coefficient and transition point x_{tr} on the profile $\bar{F}(\bar{x})$ as well as its first and second derivatives. To solve the problem numerically, we consider the class of shape functions $\bar{F}(\bar{x})$ where the slope $\bar{F}'(\bar{x})$ is approximated by a C^2 cubic spline interpolant on a set of data points (\bar{x}_i, \bar{F}'_i) , $i = 1, \dots, K$, defined as

$$\bar{x}_1 = 0, \dots, \bar{x}_j = h(j-1), \dots, \bar{x}_K = 1 \quad (15)$$

$$\bar{F}'_i = \bar{F}'(\bar{x}_i)$$

where the interval between the knots $h = 1/(K-1)$. The functional $\bar{D}_n(\bar{F})$ from Eq. (12) is replaced by the function $D_n(z)$ of vector $z = [\bar{F}'(\bar{x}_1), \dots, \bar{F}'(\bar{x}_K)]^T$. The shape function $\bar{F}(\bar{x})$ is obtained by the following integration:

$$\bar{F}(\bar{x}) = \int_0^{\bar{x}} \bar{F}'(s) ds \quad (16)$$

and belongs to the class $\bar{F}(\bar{x}) \in C^3$.

It is known that the transition process is sensitive to airfoil curvature. On concave surfaces with $\bar{F}''(\bar{x}) > 0$, Görtler vortices can compete with Tollmien-Schlichting (TS) waves. According to Eq. (7), a concave-surface supersonic airfoil generates

unfavorable pressure gradients that can lead to boundary-layer separation. To avoid uncertainty of the instability mechanism and prevent boundary-layer separation, we impose the following auxiliary constraint:

$$\max \bar{F}''(\bar{x}) \leq \varepsilon_c, \quad 0 \leq \bar{x} \leq 1 \quad (17)$$

where $\varepsilon_c \geq 0$ is a small parameter, which controls surface concavity.

The minimum drag problem is now formulated as follows. Problem B: in the class of cubic spline functions, $\bar{F}'(\bar{x}) \in C^2$, which are consistent with the sharp leading-edge conditions $\bar{F}(0) = \bar{F}(1) = 0$, knot-a-knot conditions $\bar{F}'(\bar{x}_j) = \bar{F}'_j$, $j = 1, \dots, K$, the isoperimetric constraint [Eq. (13)], and the curvature constraint [Eq. (17)] find the particular vector $z = (\bar{F}'_1, \dots, \bar{F}'_K)^T$, which minimizes \bar{D}_n given by Eq. (12).

Problem B is solved using the Schittkowski nonlinear constraint optimization algorithm.^{18,19} It applies a successive quadratic programming method to solve the nonlinear programming problem. The method, based on the iterative formulation and solution of quadratic programming subproblems, obtains subproblems by using a quadratic approximation of the Lagrangian and by linearizing the constraints.

A code based on these developments was tested by comparison between the analytical solution [Eq. (14)] and numerical solution of problem B for the airfoil shape of minimum

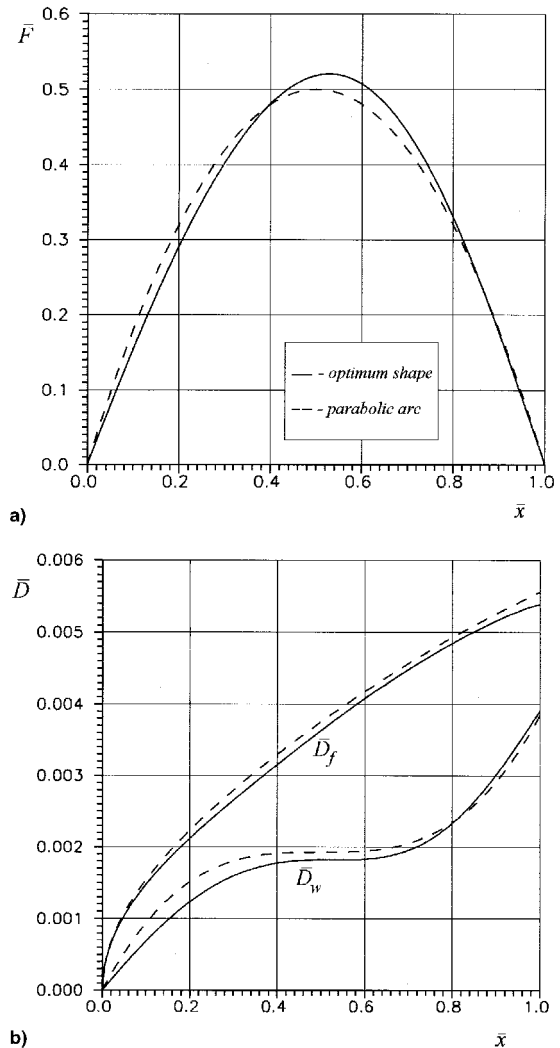


Fig. 1 a) Optimum shape for laminar flow: $M = 2$, $\varepsilon = 0.05$, and $R_c = 10^5$. b) Wave drag $\bar{D}_w(\bar{x})$, and friction drag $\bar{D}_f(\bar{x})$ distributions for laminar flow: $M = 2$, $\varepsilon = 0.05$, and $R_c = 10^5$. ----, parabolic arc; —, optimum shape.

wave drag for a given profile area ($n = 1$). The optimization process converges to the parabolic-arc shape [Eq. (14)], starting from different guesses for the vector \mathbf{z} . As an example, the numerical value of $\bar{D}_w = 1.5435 \times 10^{-2}$ was close to the analytical value $\bar{D}_w = 1.5396 \times 10^{-2}$ for Mach number $M = 2$, $\varepsilon = 0.1$, $K = 5$, and the initial shape function $\bar{F}(\bar{x}) = 0.5\bar{x}$.

A major advantage of our optimization code is its very short computational time. The optimization process including calculation of the friction drag, wave drag, and transition point is normally completed in less than 5 min, using a Pentium-90 personal computer. This allows fast parametric and tradeoff studies required for supersonic wing design.

IV. Results

We consider optimal airfoil shapes of a given area using the isoperimetric constraint [Eq. (13)] for $n = 1$. The parabolic-arc shape [Eq. (14)] is used as an initial iterate for the optimization process. The profile area is prescribed as

$$\bar{S} = \int_0^1 2\bar{x}(1 - \bar{x}) d\bar{x} = \frac{1}{3}$$

Figures 1a and 1b show optimal shape $\bar{F}(\bar{x})$ and drag distributions $\bar{D}_f(\bar{x})$, $\bar{D}_w(\bar{x})$, respectively, at $M = 2$, $\varepsilon = 0.05$, and $R_c = 10^5$. The boundary layer is laminar along the entire airfoil surface for this case. Calculations were carried out for $K = 5$

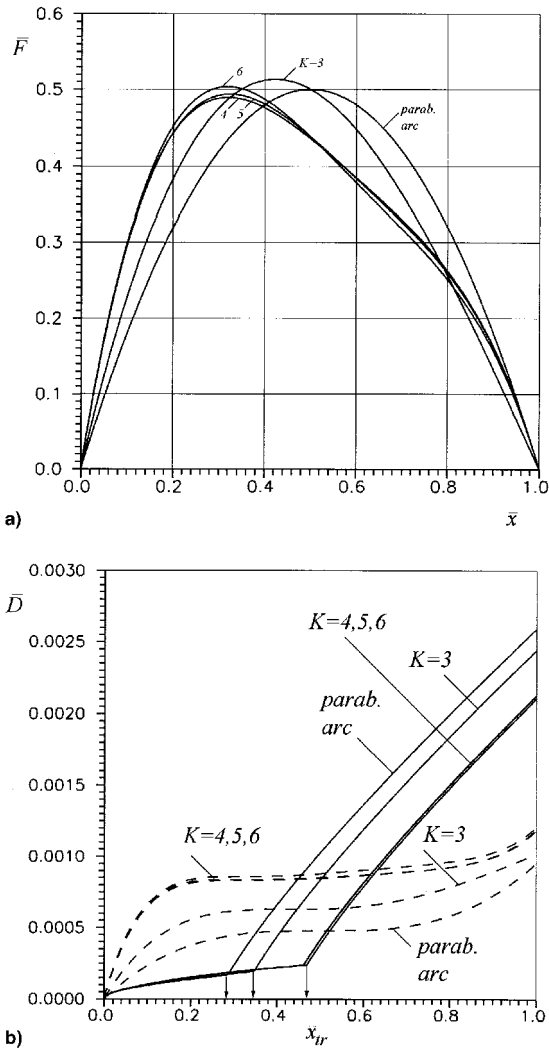


Fig. 2 a) Optimum shapes $\bar{F}(\bar{x})$ at various number of knots K : $M = 1.5$, $\varepsilon = 0.02$, and $R_c = 2 \times 10^7$. b) Friction drag $\bar{D}_f(\bar{x})$ (solid lines) and wave drag $\bar{D}_w(\bar{x})$ (dashed lines) at various number of knots K : $M = 1.5$, $\varepsilon = 0.02$, and $R_c = 2 \times 10^7$.

using the curvature constraint [Eq. (17)]. For this set of parameters, the laminar friction drag is weakly sensitive to shaping. The optimum profile (solid line) is close to the parabolic arc (dashed line), which is the minimum wave drag shape. Optimization gives a very small decrease of the total drag, namely, $\bar{D}_t = 9.2967 \times 10^{-3}$ compared to $\bar{D}_t = 9.4098 \times 10^{-3}$ of the parabolic arc. As Reynolds number and/or thickness ratio increases, the relative contribution of friction drag to the total drag decreases and the optimum profile approaches the parabolic arc. Similar trends occur for a fully turbulent boundary layer when $\bar{x}_{tr} = 0$ is not sensitive to shaping.

Airfoil shaping is more effective when transition occurs in the midchord region. According to (Eq. 7), the pressure gradient is proportional to the profile curvature. Because the transition point is very sensitive to the pressure gradient, shaping can shift the transition locus downstream and, as a result, reduce friction drag. If the friction drag is of the order of wave drag, then optimization can decrease the total drag. These transitional cases will be discussed in what follows.

Figure 2a shows optimum shapes $\bar{F}(\bar{x})$ for the profile of thickness $\varepsilon = 0.02$ at $M = 1.5$, and $R_c = 2 \times 10^7$. The transition point is predicted using the criterion $N_{\sigma} = 10$. Calculations were made for the number of knots $K = 3, 4, 5$, and 6 using the curvature constraint [Eq. (17)] with $\varepsilon_c = 10^{-5}$. The optimum shape converges with respect to K to a certain limiting shape, which is essentially different from the parabolic arc. Figure 2b illustrates distributions of friction drag $\bar{D}_f(\bar{x})$ and

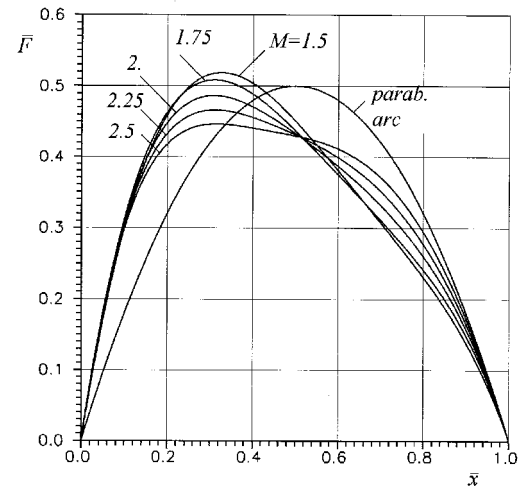


Fig. 3 Optimum shape at various Mach numbers; $\varepsilon = 0.02$, $R_c = 2 \times 10^7$, and $K = 5$.

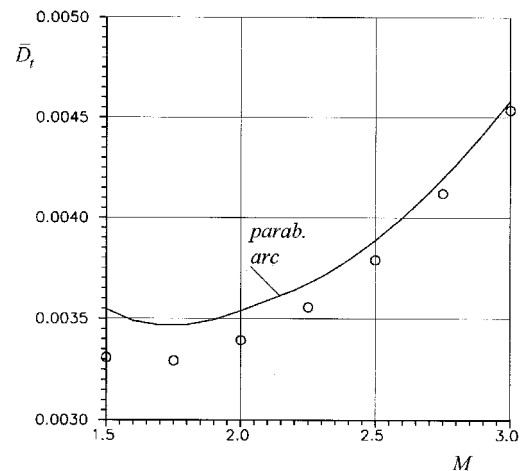


Fig. 4 Minimum drag as a function of Mach number (symbols); $\varepsilon = 0.02$, $R_c = 2 \times 10^7$, and $K = 5$.

wave drag $D_f(\bar{x})$, as well as the location of the transition point \bar{x}_t . The optimization process increases the profile curvature in the nose region. This leads to a more favorable pressure gradient. As a consequence, the transition point is shifted from $\bar{x}_t \approx 0.3$ to 0.5 , causing about a 20% decrease of friction drag. However, the new profile has higher level of wave drag compared to the parabolic arc that reduces the shaping benefit down to 7%. Figure 3 shows variation of the optimum shape vs freestream Mach number for $\varepsilon = 0.02$, $R_c = 2 \times 10^7$, and $K = 5$. The corresponding distribution of the minimum drag (symbols) and the parabolic-arc drag (solid line) are shown in Fig. 4. In spite of significant deviation of optimum profiles from the parabolic-arc shape, the drag reduction is relatively small and decreases at higher Mach numbers.

Similar calculations have been conducted with no curvature constraint [Eq. (17)]. The optimum shape was close to the convex shape when $K \leq 6$. Optimal shapes at various Reynolds numbers are shown in Fig. 5 for $M = 2$, $\varepsilon = 0.02$, and $K = 5$. The corresponding distribution of the total minimum drag (symbols) and the total drag of the parabolic-arc shape (solid line) are shown in Fig. 6. At $R_c = 1.5 \times 10^7$, optimization gives about a 10% total drag decrease compared to the parabolic arc profile. For increasing Reynolds number, the transition point is shifted upstream and becomes less sensitive to

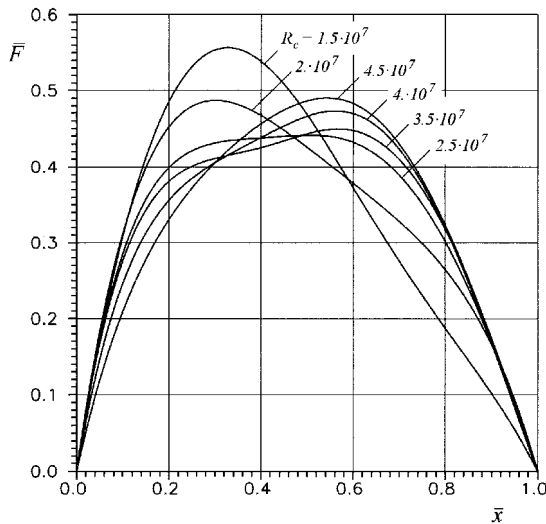


Fig. 5 Optimum shape at various Reynolds numbers; $M = 2$, $\varepsilon = 0.02$, $R_c = 2 \times 10^7$, and $K = 5$; no curvature constraint.

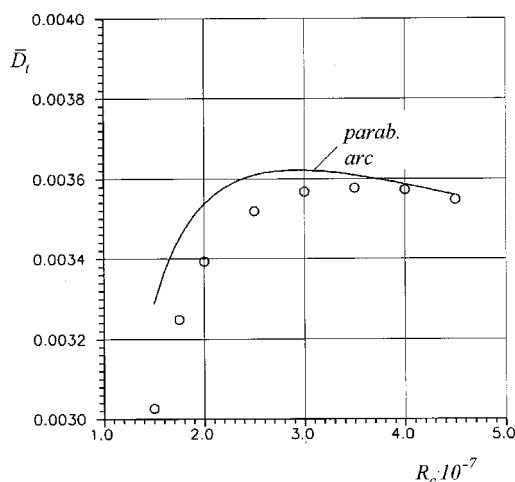


Fig. 6 Minimum drag as a function of Reynolds number (symbols); $M = 2$, $\varepsilon = 0.02$, and $K = 5$; no curvature constraint.

shaping. As a result, the drag reduction decreases and the optimum shape approaches a parabolic arc.

V. Summary

The feasibility of a procedure incorporating transition considerations in optimizing total drag has been demonstrated. The Schittkowski algorithm was used to demonstrate the approach on two-dimensional airfoils. The airfoils were approximated by cubic spline basis functions, and total drag (wave + friction) was minimized under the constraint of a fixed air-foil area. Reynolds numbers were assumed such that the airfoil was transitional, generally with the forward portion laminar and the aft portion turbulent. The transition locus was calculated using the TPM, which provides rapid computation of the TS wave amplification factor N and estimates the transition point by the e^N method. The laminar friction drag was evaluated using self-similar solutions of the boundary-layer equations. The friction drag for the turbulent portion was computed assuming a one-seventh velocity profile. With this framework, the total drag was a function of the functional x_t , the streamwise location of transition. As a validation, the algorithm gave the correct global optimum for the inviscid case, which is the parabolic arc profile. For the viscous case, significantly different locations of the maximum thickness led to only small differences in the minimum total drag. In addition, the drag reductions from the optimal inviscid parabolic profile were about 10%. Convergence with respect to the number of spline knots was achieved. Important challenges were met to reduce the effect of truncation errors in the numerical approximation of differentiations such as those used in the evaluation of the Hessian matrix. Special flexibility in the cutoff criteria for the iterations had to be built into the optimization routines, because demanding standards for convergence could not be met. Other issues regarding noisy initial iterates, e.g., from errors in geometry, propagating through the iterations as well as roundoff error, will need to be addressed in future effort. In spite of these difficulties, generalization of the approach to treat infinite yawed and swept wings accounting for suction, crossflow instabilities, and vortex drag appears feasible.

Acknowledgments

A portion of this effort was sponsored by the Air Force Office of Scientific Research, U.S. Air Force Materials Command, Contract F49620-96-C-0004. The U.S. Government is authorized to reproduce and distribute reprints for government purposes notwithstanding any copyright notation thereon. The views and conclusions herein are those of the authors and should not be interpreted as necessarily representing the official policies or endorsements, either expressed or implied, of the Air Force Office of Scientific Research or the U.S. Government.

References

1. Jones, R., "The Minimum Drag of Thin Wings in Frictionless Flow," *Journal of the Aeronautical Sciences*, Vol. 18, No. 2, 1951.
2. Shankar, V., Malmuth, N., and Cole, J., "Computational Design Procedure for 3-D Wings and Wing-Body Combinations," AIAA Paper 79-0344, 1979.
3. Kirkpatrick, S., Gelatt, C. D., and Vecchi, M. P., "Optimization by Stimulated Annealing," *Science*, Vol. 220, 1983.
4. Aly, S., Marconi, F., Ogot, M., Pelz, R., and Siclari, M., "Stochastic Optimization Applied to CFD Shape Design," AIAA Paper 95-1647, 1995.
5. Fedorov, A. V., and Malmuth, N. D., "Supersonic Airfoil Shapes of Minimum Drag," Rockwell International Science Center, SCNM96-3, Nov. 1996.
6. Balakumar, P., "Optimum Suction Distribution for Transition Control," AIAA Paper 96-1950, 1996.

⁷Ashley, H., and Landahl, M., *Aerodynamics of Wings and Bodies*, Reading, MA, 1965.

⁸Schlichting, H., *Boundary-Layer Theory*, McGraw-Hill, New York, 1968.

⁹Hayes, W. D., and Probstein, R. F., *Hypersonic Flow Theory*, Academic, New York, 1959.

¹⁰Reshotko, E., "Stability Theory as a Guide to the Evaluation of Transition Data," *AIAA Journal*, Vol. 7, No. 6, 1969, pp. 1086–1091.

¹¹Reshotko, E., "Boundary Layer Instability, Transition and Control," AIAA Paper 94-0001, 1994.

¹²Hefner, J. N., and Bushnell, D. M., "Application of Linear Stability Theory to Laminar Flow Control," AIAA Paper 79-1493, 1979.

¹³Malik, M. R., "Prediction and Control of Transition in Supersonic and Hypersonic Boundary Layers," *AIAA Journal*, Vol. 27, No. 11, 1989, pp. 1487–1493.

¹⁴Smith, A. M. O., and Gamberoni, N., "Transition, Pressure Gradient, and Stability Theory," Douglas Aircraft Co., Rept. ES 26388,

El Segundo, CA, Aug. 1956.

¹⁵Van Ingen, J. L., "A Method of Calculating Transition Region for Two-Dimensional Boundary Layers with Distributed Suction," Netherlands Wissenschaftliche Gesellschaft für Luft- und Raumfahrt, Europäischer Luftfahrtkongress, 6th, Munich, Sept. 1965.

¹⁶Fedorov, A. V., and Malmuth, N. D., "Supersonic Transitional Airfoil Shapes of Minimum Drag," AIAA Paper 97-2231, June 1997.

¹⁷Drougge, G., "Two-Dimensional Wings of Minimum Pressure Drag," *Theory of Optimum Aerodynamic Shapes*, edited by A. Miele, Academic, New York, 1965, pp. 79–86, Chap. 5.

¹⁸Schittkowski, K., "Nonlinear Programming Codes," *Lecture Notes in Economics and Mathematical Systems*, Vol. 183, Springer-Verlag, Berlin, 1980.

¹⁹Schittkowski, K., "NLPQL: A FORTRAN Subroutine Solving Constrained Nonlinear Programming Problems," *Annals of Operations Research*, edited by C. L. Monma, Vol. 5, 1986, pp. 485–500.